Evaluating LoRa Energy Efficiency for Adaptive Networks: From Star to Mesh Topologies

Moises Nunez Ochoa [*†], Arturo Guizar*, Mickael Maman * and Andrzej Duda[†]

*CEA, LETI, Minatec Campus, 17 rue des Martyrs, 38054 Grenoble, France

{moises.nunezochoa, arturo.jimenezguizar, mickael.maman}@cea.fr

[†]Univ. Grenoble Alpes, CNRS, Grenoble INP, LIG, F-38000 Grenoble France

andrzej.duda@imag.fr

Abstract—The LoRa technology has emerged as an interesting solution for low power, long range IoT applications by proposing multiple "degrees of freedom" at the physical layer. This flexibility provides either a long range at the cost of a lower data rate or higher throughput at the cost of low sensitivity, so a shorter range. In this paper, we analyze the flexibility of LoRa and propose various strategies to adapt its radio parameters (such as the spreading factor, bandwidth, and transmission power) to different deployment scenarios. We compute the energy consumption of LoRa transceivers using various radio configurations in both star and mesh topologies. Our simulation results show that in a star topology, we can achieve the optimal scaling-up/down strategy of LoRa radio parameters to obtain either a high data rate or a long range while respecting low energy consumption. In mesh networks, energy consumption is optimized by exploiting various radio configurations and the network topology (e.g., the number of hops, the network density, the cell coverage). Finally, we propose a strategy to take advantage of both star and mesh topologies.

I. Introduction

The IoT revolution offers a huge potential value in terms of improved efficiency, sustainability, and safety for industry and society. Technologies connecting IoT smart objects are extremely varied: some objects are connected through a local access point using WiFi, Zigbee, or Bluetooth, and rely on the connectivity of the access point to access a wider network; others rely on a communication infrastructure to convey the information (Cellular Access).

Over the past few years, new approaches often referred to as Low Power Wide Area (LPWA) networking technologies have emerged. These technologies define a new air interface that provides low power connectivity alternative to current generations of cellular systems (2G, 3G, and 4G), while covering large areas (typical range of $10\,\text{km}$). Wireless Personal Area Networks (WPAN) such as Zigbee and Bluetooth have been improved for power efficiency, but cannot achieve such a range. LPWA systems also aim at pushing power consumption optimization one step further.

The LPWA connectivity technology portfolio appears quite fragmented. The LPWA state-of-the-art [1] is split into two separate sub-categories. On one hand, PHY/MAC layers of the current proprietary LPWA technologies (i.e., SigFox, LoRa, Ingenu RPMA, and Weightless) typically operate in unlicensed spectrum. These "PHY based" technologies have been tailored to the specific features of IoT communications. On the other hand, there are PHY/MAC layers of standardized technologies such as Cellular IoT (e.g., EC-GSM, NB-IoT, and LTE-M) and IEEE Wireless Personal/Local Area Networks solutions (e.g., 802.15.4g, 802.15.4k, and 802.11ah [2]). These standardized technologies are mainly adaptations or extensions of existing solutions with the aims to reduce energy consumption, to reduce the cost, and/or to improve the range. For standardized cellular IoT technologies, NB-IoT is the most promising solution whereas for proprietary LPWA technologies, LoRa is widely adopted. The maturity of the solution and the opening of the system give us motivation to focus the investigation on the LoRa technology.

Several studies in the literature analyzed performance and limitations of the LoRa modulation [3] [4] [5]. Some interesting aspects of existing LoRa radios can be exploited:

- The range is several kilometers in large outdoors and hundreds of meters in large indoors. Many nodes can reach the sink node without routing over intermediate nodes. The range can be even larger (tens of kilometers) in a multi-hop scenario.
- Very low energy consumption to optimize battery lifetime.
- Network capacity to receive messages from a very large number of nodes. Using adaptive data rates and multi-channel multi-modem transceivers permits to achieve higher network capacity.
- Robustness to interference thanks to the Chirp Spread Spectrum (CSS) modulation. Since LoRa modulation is based on the spectrum spreading

principle, the signals with various spreading factors are orthogonal to each other.

Adelantado et al. studied the limitations of the LoRa technology related to capacity and network size [6]. Energy consumption comparisons with other IoT technologies were also investigated [7]. Su et al. considered power control and analyzed rate adaptation for one hop and multi hop scenarios [8]. Some authors presented experimental studies of LoRa Semtech transceivers [9] [10]. Nevertheless, the potential of an adaptive LoRa solution (i.e., in terms of spreading factor, bandwidth, transmission power, and topology) is still not well studied and exploited.

In this article, we focus on the LoRa technology and on how we can optimize energy consumption by adapting its parameters. We propose various strategies to adapt LoRa radio parameters to reduce energy consumption in various scenarios. In a star topology, we investigate the best parameters configuration that depends on the distance between the sender node and the sink node (i.e., bandwidth, spreading factor, and transmitted power). In a mesh topology, we propose various strategies depending on the network density and coverage. Finally, we compare both topologies and exploit the network architecture by boosting the use of high data rate configurations.

The article is organized as follows: Section II proposes an overview of LoRa PHY layer and LoRa modulation. Section III presents the system model and the methodology used in our analysis. Section IV and V, respectively analyze energy consumption for the star and mesh topologies by exploiting modulation, power control, and bandwidth adaptation. Section VI compares both topologies and Section VII concludes the paper.

II. LoRa Technology Overview

In Section II, we give an overview of LoRa physical layer and LoRa modulation. More information can be found in LoRa specifications [11][12] and Semtech transceiver technical documents [13] [14] [15].

A. LoRa Physical Layer

The most important LoRa physical layer parameters [14] for our study are the following:

- Carrier frequency (CF) represents the central transmission frequency used in a band. There are three bands specified in Semtech SX1276 data sheet [13]. In this article, we consider band 1 from $862\,\mathrm{MHz}$ to $1020\,\mathrm{MHz}$.
- Bandwidth (BW) is the range of frequencies available for transmission. Semtech SX1276 offers bandwidths from $7.8\,\mathrm{kHz}$ to $500\,\mathrm{kHz}$. Larger bandwidths permit higher data rates, shorter time on the air, but lower sensitivities as a result of additional noise. In this article, we analyze three values of bandwidth: $125\,\mathrm{kHz}$, $250\,\mathrm{kHz}$, and $500\,\mathrm{kHz}$, that can be easily extended to smaller values.

- Spreading Factor (SF) refers to the chirp rate used to send data over the available bandwidth. For a given SF, there are 2^{SF} chips per symbol. In this article, we consider SFs from 6 to 12 as defined in the specification [13], where SF12 gives the highest sensitivity and range, but the lowest data rate. Each decrease in SF doubles the transmission rate and halves the transmission duration and energy consumption.
- Coding Rate (CR) used by LoRa modems is a Forward Error Correction (FEC) rate. It permits the recovery of the information bits in presence of interference. Higher coding rates give more robustness against interference, but increase the time on the air. For the LoRa technology, CR can be $\frac{4}{5}$, $\frac{4}{6}$, $\frac{4}{7}$ or $\frac{4}{8}$. In this article, we consider a CR of $\frac{4}{5}$.
- The receiver sensitivity ρ_{dBm} is defined according to LoRa Semtech designer's guide [15] as follows:

$$\rho_{\mathrm{dBm}} = -174 + 10log_{10}(BW) + NF + SNR \quad (1)$$

where -174 is caused by the thermal noise effect, BW is the receiver bandwidth, NF is the receiver noise for a given hardware implementation and SNR is the minimum ratio of the desired signal power to noise that can be demodulated. SNR improvements are possible combining FEC techniques, the spread spectrum processing gain, and the performance of LoRa modulation itself. In this article, we consider the sensitivity values as shown in Table I.

TABLE I
RECEIVER SENSITIVITY [dBm] AS A FUNCTION OF THE
SPREADING FACTOR AND BANDWIDTH [13]

SF/BW	125 kHz	250 kHz	500 kHz
6	-118	-115	-111
7	-123	-120	-116
8	-126	-123	-119
9	-129	-125	-122
10	-132	-128	-125
11	-133	-130	-128
12	-136	-133	-130

B. LoRa Modulation

One major component of the LoRa technology is the modulation based on an adaptation of the chirp spread spectrum modulation. This modulation is used because of its low power transmission and channel robustness against multi-path, fading, Doppler, and in-band interference. LoRa modulation features seven orthogonal spreading factors from SF6 to SF12 to improve the spectral efficiency and the network capacity. A symbol is composed of SF bits. Each symbol changes within a window BW around the central frequency band. The

number of initial possible values of the frequency is 2^{SF}. The LoRa bandwidth of $125\,\mathrm{kHz}$ corresponds to a chip rate of $125\,\mathrm{kc/s}$ because LoRa modulation composes the spread data at a chip rate equal to the programmable bandwidth in chips per second per Hertz.

Symbol duration T_s depends on both BW and SF:

$$T_s = \frac{2^{SF}}{BW} \qquad (2)$$

The bit rate is determined as follows:

$$R_b = \frac{SF}{T_s}CR = \frac{SF.BW}{2^{SF}}CR \qquad (3)$$

Higher bit rate results from lower SF, higher BW, and a CR of $\frac{4}{5}$, at the cost of lower sensitivity and range. For example, the bit rates are $5468\,\mathrm{b/s}$ and $293\,\mathrm{b/s}$, respectively for SF6 and SF12 when considering the same BW of $125\,\mathrm{kHz}$ and a CR of $\frac{4}{5}$. Moreover, we get a shorter communication range for sensitivity of $-118\,\mathrm{dBm}$ (SF6 and $BW = 125\,\mathrm{kHz}$) compared to $-136\,\mathrm{dBm}$ (SF12 and $BW = 125\,\mathrm{kHz}$). These values are for Semtech SX1276/77/78/79 LoRa devices [13].

III. METHODOLOGY AND SYSTEM MODEL

In Section III, we describe the methodology to analyze the energy consumption for sending a $50\,\mathrm{byte}$ packet using a LoRa radio with multiple "degrees of freedom": transmitted power (i.e., $2\,\mathrm{dBm}$, $5\,\mathrm{dBm}$, $8\,\mathrm{dBm}$, $11\,\mathrm{dBm}$, and $14\,\mathrm{dBm}$ according to LoRaWAN specification [11] for EU863-870MHz band), modulation schemes (i.e., spreading factors), bandwidth, and the network topology (i.e., star and mesh). In our analysis, we do not consider protocols and scheduling.

A. Radio Propagation Model

We consider the Okumura Hata propagation model for an open rural environment operating at $868\,\mathrm{MHz}$ frequency. Thus, pathloss (PL) is given by the following expression:

$$PL_{\mathrm{Hata}} = A + Blog(d) + C \qquad (4)$$

where A, B, and C depend on the frequency and antenna height.

$$A = 69.55 + 26.16log(f_c) - 13.82log(h_b) - a(h_m) \quad (5)$$

$$B = 44.9 - 6.55log(h_b) \qquad (6)$$

where f_c is in MHz and d in km. For rural environments, $a(h_m)$ and C are given by the following expressions:

$$a(h_m) = (1.1log(f_c) - 0.7)h_m - (1.56log(f_c) - 0.8) \quad (7)$$

$$C = -4.78(log(f_c))^2 + 18.33log(f_c) - 40.98 \qquad (8)$$

For simplicity, we consider antenna heights h_m and h_b of $1\,\mathrm{m}$ and $2\,\mathrm{m}$, respectively.

B. Energy Consumption

We consider two main sources of energy dissipation:

- Energy dissipated in the transmitter E_{tx}. In this case, we consider the supply current for each transmitted power, as shown in Table II, under the following conditions: $3.3\,\mathrm{V}$ supply voltage, $25\,\mathrm{C}$ temperature, and $868\,\mathrm{MHz}$ band.

TABLE II
SUPPLY CURRENT FOR TRANSMITTER [13]

P_{tx}	$2\,\mathrm{dBm}$	$5\,\mathrm{dBm}$	$8\,\mathrm{dBm}$	$11\,\mathrm{dBm}$	$14\,\mathrm{dBm}$
I_{tx}	$24\,\mathrm{mA}$	$25\,\mathrm{mA}$	$25\,\mathrm{mA}$	$32\,\mathrm{mA}$	$44\,\mathrm{mA}$

- Energy dissipated in the receiver E_{rx}. In this case, the supply current depends on the bandwidth. Table III shows supply current for each bandwidth under the same conditions as transmission.

TABLE III
SUPPLY CURRENT FOR RECEIVER W.R.T. THE BANDWIDTH [13]

BW	$125\,\mathrm{kHz}$	$250\,\mathrm{kHz}$	$500\,\mathrm{kHz}$
I_{rx}	$10.3\,\mathrm{mA}$	$11.1\,\mathrm{mA}$	$12.6\,\mathrm{mA}$

We took all supply current values from the datasheet Semtech SX1276 [11].

IV. LoRa ADAPTATION IN THE STAR TOPOLOGY

In Section IV, we study the energy consumption to transmit a packet using various possible configurations of the spreading factor, transmission power, and bandwidth for a transceiver operating according to LoRaWAN technology. In a star topology, we consider one single hop to reach the sink node. As shown in Fig. 1, D represents the distance between a node and the sink node (e.g., base station).
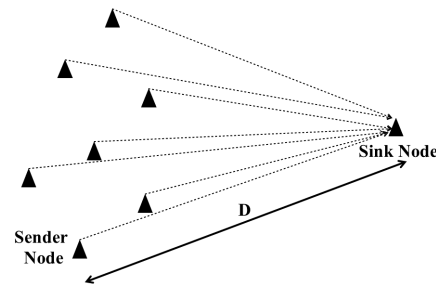

Fig. 1. Star topology.

A. Energy Consumption Depending on SF and P_{tx}

In Section IV-A, we analyze the energy consumption and the maximal reachable distance D_{max} as a function of SF and P_{tx}. In this scenario, the bandwidth is set to $125\,\mathrm{kHz}$. To do so, we have first analyzed the Maximum Coupling Loss (MCL) permitted for the link communication in Table IV, i.e., the maximum link budget permitted for each value of SF and P_{tx}. MCL

is determined according to the receiver sensitivity and transmitted power. PL_{Hata} has to be smaller than MCL to guarantee correct signal demodulation. Thus, PL_{Hata} gives the maximal distance permitted for transmission (D_{max}). In Table IV, we can observe that MCL increases when SF and P_{tx} increase. However, combinations of SF and P_{tx} give different values of energy consumption. Therefore, there is a trade-off between the range and energy consumption.

TABLE IV
MAXIMUM COUPLING LOSS OF LoRa WITH A 125 kHz BANDWIDTH.

SF/P_{tx}	2dBm	5dBm	8dBm	11dBm	14dBm
6	120	123	126	129	132
7	125	128	131	134	137
8	128	131	134	137	140
9	131	134	137	140	143
10	134	137	140	143	146
11	135	138	141	144	147
12	138	141	144	147	150

For the star topology network, we evaluate the energy consumption of a single hop as:

$$E_{\text{star}(SF,P_{\text{tx}})} = E_{\text{tx}} + E_{\text{rx}} \qquad (9)$$

where E_{tx} is the energy consumption caused by the transmission and E_{rx} caused by the reception. For this calculation, we only consider the time spend in transmission and reception, respectively. Time on air of a packet (t_{packet}) depends on SF, BW, and CR. Accordingly, energy consumption for the star topology can be expressed as follows:

$$\begin{aligned} E_{\text{star}(SF,P_{\text{tx}})} &= t_{\text{packet}} \cdot (P_{\text{tx}} + P_{\text{rx}}) \\ &= \frac{L_{\text{packet}}}{R_{\text{b}}} \cdot (P_{\text{tx}} + P_{\text{rx}}) \end{aligned} \qquad (10)$$

where L_{packet} is the size of the transmitted packet in bits. P_{tx} and P_{rx} are the consumed power according to the supply current and supply voltage for transmitter and receiver, respectively as specified in Tables II and III.
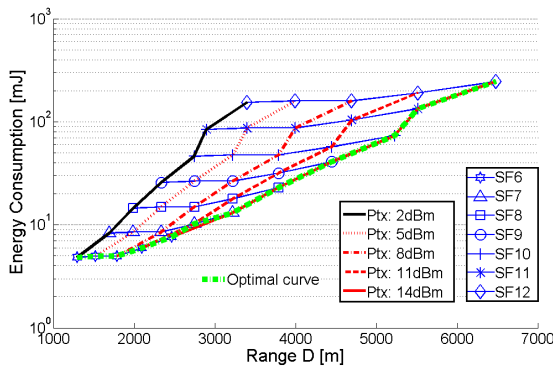
Fig. 2. Energy consumption for various configurations of SF and P_{tx} in star topology. BW is set to 125 kHz and CR to $\frac{4}{5}$.

Fig. 2 shows the energy consumption as a function of range D for different values of (SF, P_{tx}). When increasing P_{tx} (blue curves), a smooth energy consumption increase is observed for fixed SF. When switching SF ascendantly with fixed P_{tx} (red curves), energy consumption increases faster. Thus, it is preferable for increasing the range, to first increase P_{tx} and then to increment the spreading factor. For a (SF6, $P_{\text{tx}} = 2\,\text{dBm}$) configuration, Fig. 2 shows that the maximum reachable range is $D_{\text{max}} = 1.3\,\text{km}$ and energy consumption is $E = 4.8\,\text{mJ}$. Note that the maximum range ($D_{max} = 6.5\,\text{km}$) is reached using SF12 and $P_{tx} = 14\,\text{dBm}$. Beyond 6.5 km, it is not possible to establish a communication in a star topology (i.e., with a single hop).

What are the best SF and P_{tx} configurations to improve the battery lifetime?

Proposed strategy: From these results, the optimal configuration strategy to achieve lower energy consumption over distance D is shown in Fig. 3.
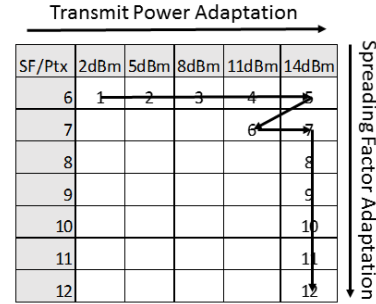
Fig. 3. Spreading factor and transmitted power adaptation strategy. Bandwidth is fixed to 125 kHz.

Thus, starting from the lowest energy consumption configuration (SF6, $P_{\text{tx}} = 2\,\text{dBm}$), the strategy is firstly to adapt the transmitted power until we reach (SF6, $P_{\text{tx}} = 14\,\text{dBm}$), then, adapt the spreading factor until reaching (SF12, $P_{\text{tx}} = 14\,\text{dBm}$). This strategy defines the optimal energy consumption curve (as shown with the green curve in Fig. 2).

B. Energy Consumption Depending on SF, P_{tx}, and BW

In Section IV-B, we extend our energy consumption analysis to three values of bandwidth: 125 kHz, 250 kHz, and 500 kHz. We follow the same approach as in Section IV-A to analyze energy consumption for 250 kHz and 500 kHz bandwidth. The optimal energy consumption curve for each BW is shown in Fig. 4.

We observe that the maximum range increases when BW decreases. This is because MCL is higher with lower BW. However, low BW comes with lower throughput and therefore, a longer time on the air, leading to higher energy consumption. Accordingly, for a range of $D < 2.6\,\text{km}$, using $BW = 500\,\text{kHz}$ permits lower energy consumption. Beyond $D = 2.6\,\text{km}$, energy consumption is similar for the three values of bandwidth. Then, BW adaptation does not have significant impact on energy
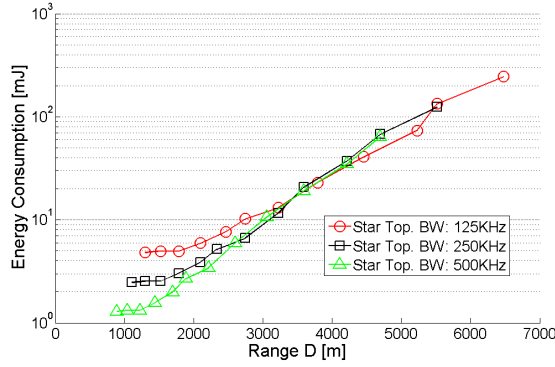
Fig. 4. Optimal energy consumption for various values of bandwidth: 125 kHz, 250 kHz, and 500 kHz in the star topology.

consumption. However, it is important for the coverage: smaller BW results in longer communication ranges.

How to exploit the multiple "degrees of freedom" (concerning SF, P_{tx}, and BW) of LoRa radio to improve the battery lifetime in a star topology?

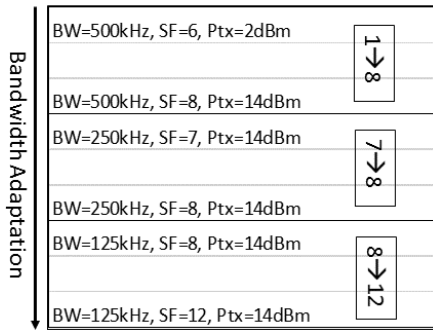**Proposed strategy:** For adapting SF, P_{tx}, and BW, Fig. 5 presents the optimal strategy.

Fig. 5. (SF, P_{tx}, BW) adaptation strategy.

The lowest energy consumption configuration is ($BW = 500$ kHz, SF6, $P_{tx} = 2$ dBm). For $BW = 500$ kHz, the box at the right side (1–>8) refers to the adaptation strategy as shown in Fig. 3. Thus, the best strategy is still first to adapt the transmitted power (up to $P_{tx} = 14$ dBm) and then, adapt the spreading factor (up to SF8). Afterward, the adaptive strategies are applied to bandwidth of 250 kHz and 125 kHz according to the boxes. For the sake of simplicity in the hardware implementation, we recommend to directly switch from $BW = 500$ kHz to $BW = 125$ kHz.

V. LoRa Adaptation in the Mesh Topology

In Section V, we analyze energy consumption to transmit a packet from a sender node to the sink node through some relay nodes. To do so, we consider a line multi-hop topology as shown in Fig. 6. We define D, the end-to-end distance (i.e., between the sender and sink node) and d, the distance between each relay.
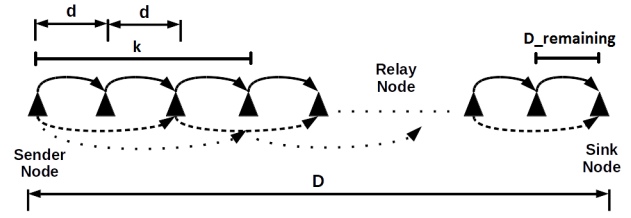

Fig. 6. Mesh topology.

We assume that one hop takes advantage of the maximal distance reachable for a given SF and P_{tx} according to the inter-relay distance granularity d. In other words, depending on the maximal range of the selected configuration, the furthest relay at distance k is reached. It is computed as follows:

$$k = \left\lfloor \frac{D_{\max}}{d} \right\rfloor .d, \tag{11}$$

where $D_{\max}$ is the maximal transmission distance for given (SF, P_{tx}). Then, n is defined as the total number of hops to reach the sink node. We denote $D_{\text{remaining}}$ as the distance between the sink node and the last relay to reach it defined as:

$$D_{\text{remaining}} = D - k. \left\lceil \frac{D}{k} \right\rceil \tag{12}$$

If $D_{\text{remaining}}$ is zero, n is computed as:

$$n = \left\lceil \frac{D}{k} \right\rceil \tag{13}$$

else, we verify if it is possible to reach the sink node from the penultimate relay by a single hop. Then, n is computed as:

$$n = \left\lceil \frac{D}{k} \right\rceil - \left\lfloor \frac{D_{\max}}{k + D_{\text{remaining}}} \right\rfloor \tag{14}$$

In Fig. 6, the maximal transmission range k of chosen (SF, P_{tx}) reaches the third relay, then the packet goes over 3 hops. In this case, it is important to evaluate what is the best relaying strategy in terms of energy consumption: one direct hop with the third node using an appropriate configuration or three hops with a more energy-efficient strategy.

Energy consumption assuming n hops to reach the sink node is:

$$E_{\text{mesh}} = \sum_{i=1}^{n} (E_{\text{tx},i} + E_{\text{rx},i}), \tag{15}$$

where $E_{\text{tx},i}$ and $E_{\text{rx},i}$ are the energy consumption of the transmitter and receiver, respectively with the current configuration of transmitted power, spreading factor, and bandwidth of hop i.

In the following simulations, the bandwidth is set to 125 kHz. The mesh topology using different spreading factors and transmitted power is analyzed as a function

of the network density and the network coverage. The network density can be modeled with the inter-relay distance d and the network coverage with the end-to-end distance D. Thus, we evaluate the energy efficiency of the LoRa mesh for various distances d between relay nodes, when D is fixed, and for various distances D from the sender node to the sink node, when d is fixed.

A. Energy Consumption Depending on Network Density

In Section V-A, we evaluate the impact of the inter-relay distance d, i.e., indirectly the network density in the mesh LoRa network. Fig. 7 shows the energy consumption depending on the inter-relay distance d, when the end-to-end distance is fixed to $10\,\mathrm{km}$. For this distance, direct communications are impossible.
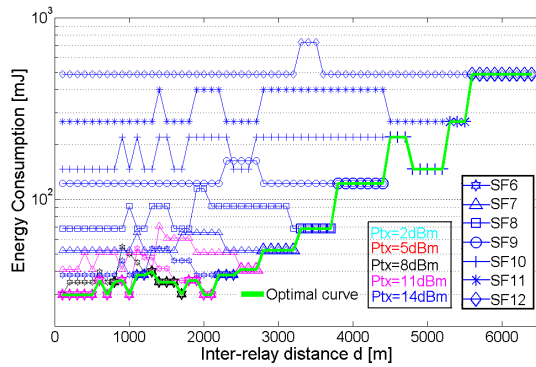

Fig. 7. Energy consumption of the mesh topology depending on inter-relay distance d when distance D between the sender node and the sink is set to $10\,\mathrm{km}$.

For inter-relay distance d higher than $6.4\,\mathrm{km}$, the link communication cannot be established: this is the limit of the LoRa range in an open rural environment. For inter-relay distance d up to $2.2\,\mathrm{km}$, we observe that the optimal configuration is SF6 (represented by a hexagon) whereas various colors show the optimal P_{tx}. For inter-relay distances larger than $2.2\,\mathrm{km}$, we observe that the optimal configuration to reach fixed distance D of $10\,\mathrm{km}$ is SF7, then SF8, then SF9, and so on until SF12 (for $D > 6.4\,\mathrm{km}$) and for all of them, P_{tx} must be set to $14\,\mathrm{dBm}$ (blue).

The green curve represents the optimal strategy for the mesh topology according to the inter-relay distance d, i.e., representing the network density. In other words, in dense networks (i.e., small d), it is better to use the lowest SF (e.g., SF6) with low power and increase progressively the transmission power when d increases. Then, when we reach the maximum permitted power (i.e., $14\,\mathrm{dBm}$), it is better to increment the spreading factor to compensate for the sparsity of the network.

Fig. 8 extends the analysis to four distances D: $5\,\mathrm{km}$, $10\,\mathrm{km}$, $15\,\mathrm{km}$, and $20\,\mathrm{km}$. Only the optimal strategy curves are displayed.
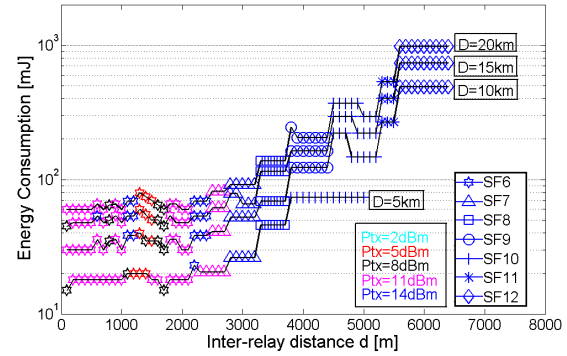

Fig. 8. Energy consumption depending on d for various ranges D.

We observe that all the curves for end-to-end distance D larger than $10\,\mathrm{km}$ follow a similar strategy with multi-hop transmissions to reach the sink. When D is $5\,\mathrm{km}$, multi-hop is useful only when the inter-relay distance is lower than $3.8\,\mathrm{km}$. Otherwise, it is better to communicate directly with (SF10, $P_{\mathrm{tx}} = 14\,\mathrm{dBm}$) configuration. Moreover, we observe that the minimum available power (i.e., $2\,\mathrm{dBm}$) is never optimal because the transmitted power is not the dominating factor of energy consumption with respect to the spreading factor adaptation and the multi-hop strategy. Moreover, our strategy always looks for the optimal number of hops reducing energy consumption. This optimization depends on the maximal transmission distance for a given (SF, P_{tx}) configuration. For instance, in the case of dense networks, where the inter-relay distance is smaller than $1\,\mathrm{km}$, it is preferable to use P_{tx} of $11\,\mathrm{dBm}$ rather than $2\,\mathrm{dBm}$ because the larger $D_{\max}$, the smaller the number of hops, thus reducing energy consumption. We conclude that depending on the inter-relay distance in dense networks, the best strategy consists in using the lowest SF and the transmission power that optimize the number of hops to reach the sink. However, when the network becomes sparser, we use a scaling up strategy on SF with the maximum permitted power (e.g., $14\,\mathrm{dBm}$).

B. Energy Consumption Depending on Network Coverage

In Section V-B, we evaluate the impact of end-to-end distance D, i.e., indirectly the cell coverage on energy consumption. For this purpose, we have extended the analysis to the case when d is fixed and D varies. In this scenario, we aim to evaluate the total energy consumption needed to transmit a packet to reach the sink node located at D meters from the sender node. To do so, we consider transmissions through the optimal relay nodes with the optimal (SF, P_{tx}) configurations.

In Fig. 9, we present the energy consumption as a function of end-to-end distance D for various inter-relay distances d (i.e., $0.1\,\mathrm{km}$, $0.5\,\mathrm{km}$, $1\,\mathrm{km}$, $2\,\mathrm{km}$, $3\,\mathrm{km}$, $4\,\mathrm{km}$, $5\,\mathrm{km}$, and $6\,\mathrm{km}$).
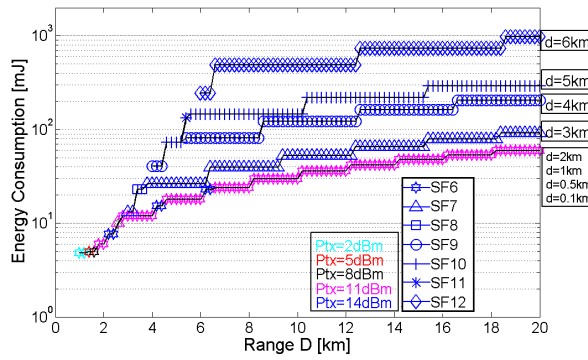
Fig. 9. Energy consumption depending on range D for various inter-relay distances d.

For an inter-relay distance smaller than $d < 2\,\text{km}$, we observe similar energy consumption as using the optimal SF configuration (i.e., SF6, variable P_{tx}). For $d > 2\,\text{km}$, we observe that the optimal SF configurations are SF7, SF9, SF10, SF12 for $d = 3\,\text{km}$, $4\,\text{km}$, $5\,\text{km}$, $6\,\text{km}$, respectively. Moreover, we observe that for sparse networks (i.e., $d > 2\,\text{km}$), the number of hops proportionally increases when the cell coverage increases in a multiple of the inter-relay distance. In these intervals, the radio configuration is the same and energy consumption remains constant. For instance, when $d = 6\,\text{km}$, the sink is directly reached when D is smaller that $6.4\,\text{km}$, with 2-hops when D is between 6.4 and $12.4\,\text{km}$, with 3-hops when D is between 12.4 and $18.4\,\text{km}$ and so on.

How to take advantage of the network architecture by boosting the use of high data rate configurations?

Proposed strategy: The optimal strategy to achieve the lowest energy consumption as a function of inter-relay distance d is shown in Fig. 10.
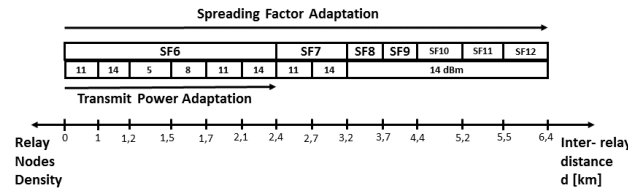

Fig. 10. (SF, P_{tx}) adaptation strategy.

For small inter-relay distances (i.e. $d < 1.2\,\text{km}$), as the number of relay nodes is large, the best strategy is to maximize the reachable distance of each hop with a configuration using the highest transmitted power (i.e., 11 or $14\,\text{dBm}$) and the smallest spreading factor (i.e., SF6). From $d = 1.2\,\text{km}$ to $d = 2.4\,\text{km}$, the strategy is to adapt the transmitted power from $5\,\text{dBm}$ up to $14\,\text{dBm}$. Finally, from $d = 2.4\,\text{km}$ to $d = 6.4\,\text{km}$, the strategy is to adapt SF: from (SF7, $P_{\text{tx}} = 14\,\text{dBm}$) to (SF12, $P_{tx} = 14\,\text{dBm}$) configurations.

VI. Network Topology Impact: Star vs. Mesh

In Section VI, we compare the energy consumption of star and mesh topologies. In the star topology, we

consider the optimal configuration to achieve low energy consumption and the maximum range, that results in a fair comparison between both topologies. In Fig. 11, we observe the energy consumption of a Lora mesh network using a BW of $125\,\text{kHz}$ for various network densities (i.e., inter-relay distances d) and the optimal energy consumption curves for the star topology for BW of $125\,\text{kHz}$, $250\,\text{kHz}$, and $500\,\text{kHz}$.
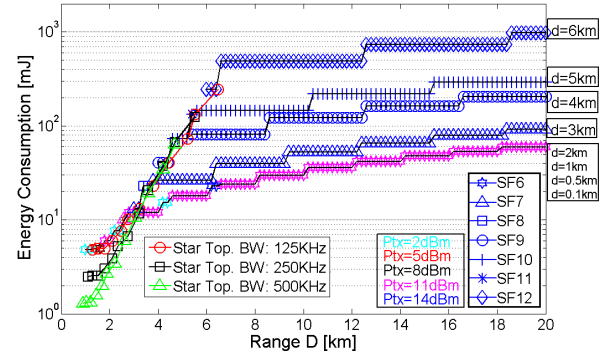

Fig. 11. Energy consumption in star and mesh topologies.

We observe that up to 3 km, the energy consumption of the star topology is the lowest. Beyond $D = 3\,\text{km}$, the mesh topology becomes interesting.

How to jointly exploit the multiple "degrees of freedom" (concerning SF, P_{tx}, and BW) of LoRa radio and the network topology to improve the battery lifetime?

Proposed strategy: The optimal strategy exploiting both topologies is shown in Fig. 12. Depending on inter-relay distance d, we propose an adaptive strategy over distance D passing from the star to the mesh topology. In the case of a dense network (i.e., $d < 2.4\,\text{km}$), we propose a star strategy as described in Section IV.B when $D < 3.0\,\text{km}$. Beyond $3.0\,\text{km}$, a mesh strategy with (SF6, $P_{\text{tx}} = 11\,\text{dBm}$) configuration becomes more efficient to reach the sink node. For $2.4\,\text{km} < d < 3.2\,\text{km}$, the best configuration consists in following the star strategy up to $D = 3.2\,\text{km}$. Then, we recommend to pass to a mesh strategy. A similar behavior is observed when increasing d up to $6.4\,\text{km}$.

VII. Conclusion and Future work

In this article, we investigate the energy consumption for sending a $50\,\text{byte}$ packet with various LoRa configurations for star and mesh topologies. The goal is to exploit the LoRa technology by adapting its parameters (i.e., spreading factor, bandwidth, and transmitted power). We compute energy consumption based on the transceiver data sheet Semtech SX1276.

For the star topology, we observe that increasing SF has a more significant impact on energy consumption than increasing P_{tx}, that also makes the communication

	500kHz			250kHz		125kHz					(mesh)	d [km]
star	SF6	SF7	SF8	SF7	SF8	SF8	SF9	SF10	SF11	SF12	SF12	6,4
	2 5 8 11 14	11 14	14	14	14	14					14	
	SF6	SF7	SF8	SF7	SF8	SF8	SF9	SF10	SF11		SF11	5,5
	2 5 8 11 14	11 14	14	14	14	14					14	5,2
	SF6	SF7	SF8	SF7	SF8	SF8	SF9	SF10			SF10	
	2 5 8 11 14	11 14	14	14	14	14					14	4,4
	SF6	SF7	SF8	SF7	SF8	SF8	SF9				SF9	
	2 5 8 11 14	11 14	14	14	14	14					14	3,7
	SF6	SF7	SF8	SF7	SF8	SF8					SF8	
	2 5 8 11 14	11 14	14	14	14	14					14	3,2
	SF6	SF7	SF8	SF7	SF8						SF7	
	2 5 8 11 14	11 14	14	14	14						14	2,4
	SF6	SF7	SF8	SF7							SF6	
	2 5 8 11 14	11 14	14	14							11	

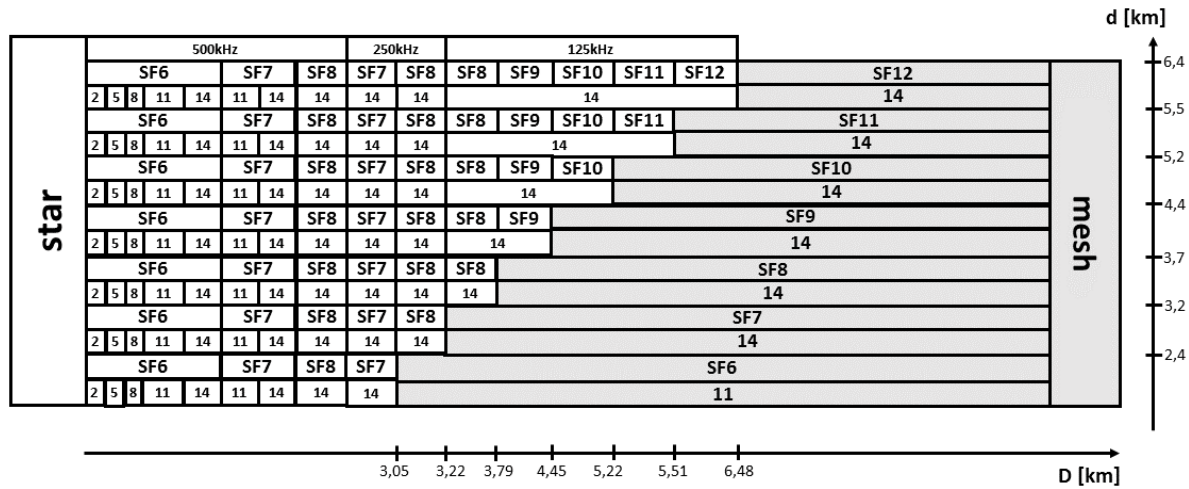D [km]: 3,05 3,22 3,79 4,45 5,22 5,51 6,48

Fig. 12. Topology adaptation strategy.

range longer. Ththe best strategy is firstly to adapt the transmission power and then to increment the spreading factor to obtain the optimal energy consumption. When the bandwidth is considered, our results show that the optimal energy consumption is for $BW = 500\,\text{kHz}$ up to a range of $3\,\text{km}$. Beyond $3\,\text{km}$, we adapt BW according to the data rate and range constraints.

For the mesh topology, the energy consumption is optimized by exploiting different radio configurations and the network topology (e.g., the number of hops, the network density, the cell coverage). In dense networks, the proposed strategy consists of setting the spreading factor to SF6 and progressively increasing the transmitted power with the inter-relay distance. In the case of sparse networks, we recommend to adapt SF until reach the (SF=12, $P_{\text{tx}} = 14\,\text{dBm}$) configuration.

According to the topology comparison, we show that a global strategy exploiting both topologies exists and the trade-off between the star and mesh strategies depends on end-to-end distance D (i.e., the network coverage) and inter-relay distance d (i.e. the network density). Adapting the topology and the LoRa radio parameters permits to maintain low energy consumption and to extend the range of communication.

In the future work, we plan to maximize the overall capacity of the LoRa mesh network by exploiting the orthogonality of various spreading factors and the spatial reuse of the communication. This optimization requires MAC/routing protocols and an accurate interference model with a realistic network simulator, especially to consider the hidden and exposed terminal problems present in mesh topologies.

ACKNOWLEDGMENTS

REFERENCES

[1] U. Raza, P. Kulkarni, and M. Sooriyabandara, "Low power wide area networks: An overview," *IEEE Communications Surveys Tutorials*, vol. PP, no. 99, pp. 1–1, 2017.

[2] E. Khorov, A. Lyakhov, A. Krotov, and A. Guschin, "A survey on ieee 802.11ah: An enabling networking technology for smart cities," *Computer Communications*, vol. 58, 2015. Special Issue on Networking and Communications for Smart Cities.

[3] C. Goursaud and J. M. Gorce, "Dedicated networks for iot: Phy / mac state of the art and challenges," *EAI Endorsed Transactions on Internet of Things*, vol. 15, 10 2015.

[4] K. Mikhaylov, . J. Petaejaejaervi, and T. Haenninen, "Analysis of capacity and scalability of the lora low power wide area network technology," in *European Wireless 2016; 22th European Wireless Conference*, pp. 1–6, May 2016.

[5] K. Mikhaylov, J. Petäjäjärvi, J. Haapola, and A. Pouttu, "D2D communications in lorawan low power wide area network: From idea to empirical validation," *CoRR*, vol. abs/1703.01985, 2017.

[6] F. Adelantado, X. Vilajosana, P. Tuset, B. Martinez, J. MELIA-SEGUI, and T. Watteyne, "Understanding the limits of lorawan," *IEEE Communications Magazine*, June 2017.

[7] E. Morin, M. Maman, R. Guizzetti, and A. Duda, "Comparison of the device lifetime in wireless networks for the internet of things," *IEEE Access*, vol. PP, no. 99, pp. 1–1, 2017.

[8] Y. Su, Y. Zhu, H. Mo, J.-H. Cui, and Z. Jin, "A joint power control and rate adaptation {MAC} protocol for underwater sensor networks," *Ad Hoc Networks*, vol. 26, pp. 36 – 49, 2015.

[9] M. Bor, J. Vidler, and U. Roedig, "Lora for the internet of things," in *Proceedings of the 2016 International Conference on Embedded Wireless Systems and Networks*, EWSN '16, (USA), pp. 361–366, Junction Publishing, 2016.

[10] T. Petric, M. Goessens, L. Nuaymi, L. Toutain, and A. Pelov, "Measurements, performance and analysis of lora fabian, a real-world implementation of lpwan," in *2016 IEEE 27th Annual International Symposium on Personal, Indoor, and Mobile Radio Communications (PIMRC)*, pp. 1–7, Sept 2016.

[11] N. Sornin, M. Luis, T. Eirich, T. Kramp, and O.Hersent, "Lo-rawan specification v1.0 2015, lora alliance," 2015.

[12] N. Sornin, M. Luis, T. Eirich, T. Kramp, and O.Hersent, "Lo-rawan specification v1.0.2," 2016.

[13] Semtech, "Sx1276 137 mhz to 1020 mhz low power long range transceiver," 2015.

[14] Semtech, "Application note an1200.22 lora modulation basics," 2015.

[15] Semtech, "Sx12172/3/6/7/8 application note an1200.13 modem designer's guide," 2013.